



**HAL**  
open science

## The Black Hole Universe (BHU)

Enrique Darkcosmos.Com Gaztanaga

► **To cite this version:**

| Enrique Darkcosmos.Com Gaztanaga. The Black Hole Universe (BHU). 2021. hal-03344159v2

**HAL Id: hal-03344159**

**<https://hal.science/hal-03344159v2>**

Preprint submitted on 10 Oct 2021 (v2), last revised 5 Apr 2022 (v5)

**HAL** is a multi-disciplinary open access archive for the deposit and dissemination of scientific research documents, whether they are published or not. The documents may come from teaching and research institutions in France or abroad, or from public or private research centers.

L'archive ouverte pluridisciplinaire **HAL**, est destinée au dépôt et à la diffusion de documents scientifiques de niveau recherche, publiés ou non, émanant des établissements d'enseignement et de recherche français ou étrangers, des laboratoires publics ou privés.

# The Black Hole Universe (BHU)

Enrique Gaztañaga<sup>\*</sup>

*Institute of Space Sciences (ICE, CSIC), 08193 Barcelona, Spain  
Institut d'Estudis Espacials de Catalunya (IEEC), 08034 Barcelona, Spain*

October 9, 2021

## ABSTRACT

Recent observations show that cosmic expansion is dominated by an effective cosmological constant. This means that we live inside a trapped surface, which corresponds to a Black Hole (BH) event horizon. We show that such Black Hole Universe (BHU) is also a solution to classical GR, where two nested FLRW metrics are connected by a BH event horizon. Observed CMB anomalies are consistent with these idea. The BHU solution can be used to model our Universe or a stellar BH inside. Observed BHs (and possibly BHs making the Dark Matter, DM) could be made of such BHUs. A BHU can originate by kinetic damping of a field into a false vacuum in an expanding background, such as cosmic inflation or a supernova explosion. In comoving coordinates the BHU is expanding while in Schwarzschild coordinates it is asymptotically static. Such frame duality allows for a Perfect Cosmological Principle where spacetime can be homogeneous both in space and time, in better agreement with relativity.

**Key words:** Cosmology: dark energy, cosmic background radiation, cosmological parameters, early Universe, inflation

## 1 INTRODUCTION

BB, DM, Dark Energy (DE),  $\Lambda$  and BHs are puzzles we don't understand at any fundamental level. The corresponding GR solutions seem to involve singularities that make no physical sense. Many theorist interpret mathematical singularity theorems as evidence that no other solutions can possibly exist and that solution to these puzzles require a theory of Quantum Gravity. But this is far from settle (Dadhich 2007) and it is outside the scope of our paper. That a non singular version of such solutions exist is clear from direct observations. Here we elaborate over a well known example of non singular classical solution to GR: the Bubble Universes. A domain wall, or thin bubble, connects a region of false vacuum, with de Sitter (dS) space inside, with empty space. These solutions are not very appealing because they have no regular matter and require a surface term (or bubble tension  $\sigma \neq 0$ ) to artificially glue dS and SW metrics discontinuity (e.g. see Blau et al. 1987; Aguirre & Johnson 2005). Our BHU proposal is a new type of Bubble Universe with a FLRW interior (including regular matter) and no bubble or surface term ( $\sigma = 0$ ).

We might never know how the BB or inflation started, but this does not prevent us from using them as the standard cosmological model to interpret observations. Something similar happens with BHs. For the same reason, we don't need to specify a particular formation mechanism to consider the BHU as an alternative to the BB and BH paradigms. In §2.1 and 6.3, we give some ideas on how a BHU could form. But our scope and focus here is not on the formation mechanism but to show that a new classical non-singular GR solutions exist and hopefully it can help us understanding the above puzzles.

A Schwarzschild BH metric (BH.SW) represents a singular object of mass  $M$ . The BH event horizon  $r_{SW} \equiv 2GM$  prevent us from

interacting with the inside (which makes BHs good potential Dark Matter candidates). Physically, a singular point does not make any sense.<sup>1</sup> But objects with mass and sizes matching  $r_{SW}$  have been observed. What is the metric inside? What happens when they accrete matter or when two BHs merge? Do BHs grow and co-evolve with galaxies (e.g. Kormendy & Ho 2013)? Do observed BH form in stellar collapse or are they seeded by primordial BHs? How do primordial BH form (e.g. Kusenko 2020)? Most of these modelings assume the BH.SW solution, but can we actually answer any of this if we do not have a physical model for the BH interior?

Here, we look for an alternative solution to the BH.SW interior, defined as a non singular classical object of size  $r_{SW}$  which reproduces the BH.SW metric for the outside  $r > r_{SW}$ . A physical BH of size  $r = r_{SW}$  and mass  $M$ , has a density:

$$\rho_{BH} = \frac{M}{V} = \frac{3r_{SW}^{-2}}{8\pi G} = \frac{3M^{-2}}{32\pi G^3}. \quad (1)$$

This is more compact than any form of regular matter (Buchdahl 1959). The highest known density for a stellar object is that of a Neutron star, which has the density of an atomic nucleus, but is still a few times larger than  $r_{SW}$ . To achieve such a high density for a perfect fluid, the radial pressure inside a BH needs to be negative (Brustein & Medved 2019 and references therein). Cosmologist are used to this type of fluids, which are called Quintessence, Inflation or Dark Energy (DE). So, could the inside of a BH be DE? Mazur & Mottola (2015) have argued that the same DE repulsive force that causes cosmic acceleration could also prevent the BH collapse, resulting in the so call gravastar solution. The simplest DE is the

<sup>1</sup> This is why it took Newton over 20 years to publish the inverse square law of gravity. He did not need to solve Quantum Gravity to address such singularity, but he had to (re) invent integration (darkcosmos.com).

<sup>\*</sup> E-mail: gaztanaga@gmail.com

ground state  $\rho_{vac} \equiv V_0(\varphi)$  of a scalar field  $\varphi(x)$ . When such DE is constant both as a function of space and time, it is equivalent to  $\Lambda$ . [Gaztañaga \(2021\)](#) have argued that a constant vacuum energy does not gravitate, but a false vacuum (FV) discontinuity does.

Here, we look for a classical BH solution defined by a spatial discontinuity at the event horizon. This requires non-static solutions with radial fluid velocity  $u \neq 0$  relative to the outside SW observer. The two key questions we want to address here are: What are possible metrics for the inside of such a physical BH? What is the meaning of the BH mass  $M$  measured by an outside SW observer, like us?

We find a new solution to these questions, which we call the BHU metric. We will also explore the idea that our Universe corresponds to such BHU solution. As the universe expands  $H$  tends to  $H_\Lambda$  which corresponds to a trapped surface  $r_\Lambda = 1/H_\Lambda$ , just like the event horizon of a BH. Moreover, the density of our universe in that limit is  $\rho = 3H_\Lambda^2/8\pi G$  which exactly corresponds to that of a BH, in Eq.1 for  $r_{SW} = r_\Lambda$ . This is not just a coincidence as advocated by some scientist ([Landsberg 1984](#); [Knutsen 2009](#)). It directly indicates that we actually live inside a very massive physical BH. It also tells us what is the metric inside a BH: our Universe is the only object whose interior we know and has the density of a BH. We will explicitly show that such BHU is a solution to classical GR.

The idea that the universe might be generated from the inside of a BH is not new and has extensive literature. [Easson & Brandenberger \(2001\)](#) and [Oshita & Yokoyama \(2018\)](#) present a good summary of past and recent literature which mostly focused in dS metric with a dual role of the BH interior and an approximation for our universe. Many of the formation mechanisms involve some modifications or extensions of GR, often motivated by quantum gravity or string theory. This is what we try to avoid here ([Ellis & Silk 2014](#)). There are also some examples (e.g. [Daghigh et al. 2000](#)) which presented models within the scope of a classical GR and classical field theory with FV interior similar to our BH.fv solution here. These models are affected by the no-go theorem, such as [Galtsov & Lemos \(2001\)](#), that state that no smooth solution to  $\varphi(x)$  can interpolate between dS and SW space. But this is not an issue for our solution for two reasons. First, the external asymptotic space is really SW+dS or FLRW (a BH is a perturbation within a FLRW metric), where solutions do exist (e.g. [Dymnikova 2003](#)). Second, we do not need  $\varphi(x)$  to smoothly transit between metrics:  $\varphi(x)$  is trapped in a FV, which is discontinuous by nature.

The above solutions provide support to the idea that our universe could be inside a BH, but they are too simplistic, as they don't contain any matter or radiation. Can these ideas be extended to the FLRW metric? Several authors have grasped the idea and speculated that the FLRW metric could be the interior of a BH ([Pathria 1972](#); [Good 1972](#); [Popławski 2016](#); [Zhang 2018](#)). But these were incomplete ([Knutsen 2009](#)) or outside classical GR. [Stuckey \(1994\)](#) found that an inside dust dominated FLRW metric could be joined to an outside BH.SW metric. This provides a new exact solution to GR which is a good precedent to our BH.u solution (in §4.2). Here we independently extend and re-interpreted this solution. First we have included radiation and a  $\Lambda$  term (or a FV vacuum), which is to understand the dual role of  $\rho_\Lambda$  as a boundary and a BH event horizon. We also interpret the outside BH.SW solution as perturbation in an external FLRW and explore the physical BH and cosmological interpretation of such solution. We also give some new ideas on how such BHU could form.

The BHU solution is quite different from that of [Smolin \(1992\)](#), who speculated that all final (e.g. BH) singularities 'bounce' or tunnel to initial singularities of new universes. Here we propose the opposite, that such mathematical singularities are not needed to explain the

physical world. As stated by [Ellis \(2008\)](#), the concept of physical infinity is not a scientific one if science involves testability by either observation or experiment. The BHU model can avoid the initial causal and entropy paradoxes ([Dyson et al. 2002](#); [Penrose 2006](#)) because of its origin within a larger expanding spacetime.

In §2 we present the GR field equations of a perfect fluid for homogeneous solutions: a FV and an expanding FLRW universe. In §3 we give a brief introduction to the general case of in-homogeneous solutions with spherical symmetry in proper SW coordinates. The FLRW solution can also be expressed in these SW coordinates. This duality is a key ingredient to find our new solution for a physical BH interior in §4. As far as we know this is a new result. In §5 we discuss how to apply these solutions to our universe. We end with a summary and a discussion of observational windows to test the BHU.

## 2 HOMOGENEOUS SOLUTIONS

We will solve Einstein's field equations (EFE) [Padmanabhan \(2010\)](#):

$$G_{\mu\nu} + \Lambda g_{\mu\nu} = 8\pi G T_{\mu\nu} \equiv -\frac{16\pi G}{\sqrt{-g}} \frac{\delta(\sqrt{-g}\mathcal{L})}{\delta g^{\mu\nu}}, \quad (2)$$

where  $G_{\mu\nu} \equiv R_{\mu\nu} - \frac{1}{2}g_{\mu\nu}R$  and  $\mathcal{L}$  is the matter Lagrangian. For perfect fluid in spherical coordinates:

$$T_{\mu\nu} = (\rho + p)u_\mu u_\nu + p g_{\mu\nu} \quad (3)$$

where  $u_\nu$  is the 4-velocity ( $u_\nu u^\nu = -1$ ),  $\rho$ , and  $p$  are the energy-matter density and pressure. This fluid is in general made of several components, each with a different equation of state  $p = \omega\rho$ . In general, for a fluid moving with relative radial velocity  $u$  with  $u^\nu = (u^0, u, 0, 0)$ , we have  $u_0^2 = -g_{00}(1 + g_{11}u^2)$  and:

$$\begin{aligned} T_0^0 &= -\rho - u^2(\rho + p)g_{11} & ; & & T_1^1 &= p + u^2(\rho + p)g_{11} \\ T_0^1 &= (\rho + p)u_0u & ; & & T_2^2 &= T_3^3 = p \end{aligned} \quad (4)$$

For a comoving observer  $u = 0$ . The outside manifold  $\mathcal{M}_{out}$  is empty space so the outside metric  $g_{out}$  is the BH.SW. Because the inside  $\mathcal{M}_{in}$  is causally disconnected,  $\mathcal{M}_{out}$  acts like a boundary condition ([Gaztañaga 2021](#)). Given some  $\rho$  and  $p$  inside  $r_{SW}$ , we will solve EFE inside to find  $g_{in}$ . To impose the boundary at  $r_{SW}$  we will use the same (proper) SW outside coordinate frame (that is not comoving with the fluid). This will result in solutions for  $\mathcal{M}_{in}$  that are not static. We will verify [Israel \(1967\)](#) conditions to check that the joint manifold  $\mathcal{M} = \mathcal{M}_{in} \cup \mathcal{M}_{out}$  is also a solution to EFE without any surface terms (see §4.3).

### 2.1 Scalar field in curved space-time

Consider a minimally coupled scalar field  $\varphi = \varphi(x_\alpha)$  with:

$$\mathcal{L} \equiv K - V = -\frac{1}{2}\partial_\alpha\varphi\partial^\alpha\varphi - V(\varphi) \quad (5)$$

The Lagrange equations are:  $\bar{\nabla}^2\varphi = \partial V/\partial\varphi$ . We can estimate  $T_{\mu\nu}(\varphi)$  from its definition in Eq.2 to find:

$$T_{\mu\nu}(\varphi) = \partial_\mu\varphi\partial_\nu\varphi + g_{\mu\nu}(K - V) \quad (6)$$

comparing to Eq.3:

$$\rho = K + V \quad ; \quad p = |K| - V \quad (7)$$

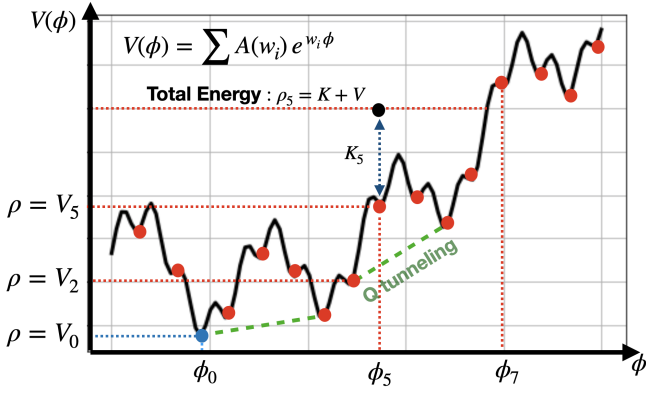


**Figure 1.** The potential  $V(\phi)$ , of a classical scalar field  $\phi(x)$ , made of the superposition of plane waves. A configuration with total energy:  $\rho_5 = K_5 + V_5$  (black dot at  $\phi_5$ ) can lose its kinetic energy  $K_5$  during expansion (e.g. a supernova explosion or an expanding background) due to Hubble damping and relax into one of the static ( $K = 0$ ) ground state (or FV)  $\rho_5 = V_5 \equiv V(\phi_5)$  (red dots). This can generate a Black Hole (BH.fv) and regular matter from reheating. Each FV has an energy excess  $\Delta_i \equiv V_i - V_0$  over the true vacuum at  $V_0$  (blue dot). Quantum tunneling (dashed lines) could allow  $\phi$  to jump between FV, resulting in BH evaporation and new matter/radiation.

In general we can have  $p_{\parallel} \neq p_{\perp}$  for non canonical scalar fields (see Eq.5 in Díez-Tejedor & Feinstein 2006 for further details). The stable solution corresponds to  $p = -\rho \equiv -\rho_{vac}$ :

$$\bar{\nabla}^2 \varphi = \partial V / \partial \varphi = 0 \quad ; \quad \rho \equiv \rho_{vac} = -p = V(\varphi) = V_i \quad (8)$$

where  $\varphi$  is trapped in the true minimum  $V_0$  or some false vacuum (FV) state  $V_i = V_0 + \Delta$ . The situation is illustrated in Fig.1. Consider a localized field with some fixed total energy  $\rho = K + V$  (black dot labeled  $\rho_5$  in the figure). In an expanding background (such a supernovae explosion or Inflation) the field can rapidly lose its kinetic energy ( $K_5$ ), due to Hubble damping, and end up trapped inside some FV ( $V_5$ ). If the outside background is at a lower FV, this will generate an expanding BH of type BH.fv, as we will discuss in §4.1. This could be the final outcome of stellar collapse, or the start of some new cosmic inflation, avoiding the traditional BB or BH.SW singularities. Because additional FV structure can exist within a given FV, the same Hubble damping can form a BH.fv inside a larger BH.fv. When  $K$  is not fully damped, the classical reheating mechanism around a FV could also be a source of matter/radiation. This could turn a BH.fv into BH.u (see §4.2). Quantum tunnelling can result in a phase transition or vacuum evaporation, which can also be a source of matter/radiation and new BH.fv.

## 2.2 The FLRW metric in comoving spherical coordinates

The FLRW metric in comoving coordinates  $\xi^\alpha = (\tau, \chi, \delta, \theta)$ , corresponds to an homogeneous and isotropic space:

$$ds^2 = f_{\alpha\beta} d\xi^\alpha d\xi^\beta = -d\tau^2 + a(\tau)^2 \left[ d\chi^2 + \chi^2 d\omega_k^2 \right] \quad (9)$$

where we have introduced the solid angle:  $d\omega_k \equiv \text{sinc}(\sqrt{k}\chi) d\omega$  with  $d\omega^2 = \cos^2 \delta d\theta^2 + d\delta^2$  and  $k$  is the curvature constant  $k = \{+1, 0, -1\}$ . For the flat case ( $k = 0$ ) we have  $d\omega_k^2 = d\omega^2$ . The scale factor,  $a(\tau)$ , describes the expansion/contraction as a function of comoving or cosmic time  $\tau$  (proper time for a comoving observer).

For a comoving observer, the time-radial components are:

$$\begin{pmatrix} T_{00} & T_{10} \\ T_{01} & T_{11} \end{pmatrix} = \begin{pmatrix} \rho(\tau) & 0 \\ 0 & p(\tau)a^2 \end{pmatrix} \quad (10)$$

i.e.  $u = 0$  in Eq.4. The solution to EFE in Eq.2 is:

$$3 \left( \frac{\ddot{a}}{a} \right) = R_{\mu\nu} u^\mu u^\nu = \Lambda - 4\pi G(\rho + 3p) \quad (11)$$

$$H^2 \equiv \left( \frac{\dot{a}}{a} \right)^2 = H_0^2 \left[ \Omega_m a^{-3} + \Omega_R a^{-4} + \Omega_k a^{-2} + \Omega_\Lambda \right] \quad (12)$$

$$\rho_\Lambda \equiv \rho_{vac} + \frac{\Lambda}{8\pi G} \quad (13)$$

$$\rho_c \equiv \frac{3H^2}{8\pi G} \quad ; \quad \Omega_X \equiv \frac{\rho_X}{\rho_c(a=1)} \quad (14)$$

where  $\Omega_m$  (or  $\rho_m$ ) represent the matter density today ( $a = 1$ ),  $\Omega_R$  is the radiation,  $\rho_{vac}$  represents vacuum energy:  $\rho_{vac} = -p_{vac} = V(\varphi)$  in Eq.8, and  $\rho_\Lambda = -p_\Lambda$  is the effective cosmological constant density. Note that  $\Lambda$  (the raw value) is always constant, but  $\rho_\Lambda$  (effective value) can change if  $\rho_{vac}$  changes. Given  $\rho$  and  $p$  at some time, we can use the above equations to find  $a = a(\tau)$  and determine the metric in Eq.9. Recent observations show that the expansion rate today is dominated by  $\rho_\Lambda$ . This indicates that the FLRW metric lives inside a trapped surface  $r_\Lambda \equiv 1/H_\Lambda = (8\pi G \rho_\Lambda / 3)^{-1/2}$ , which behaves like the interior of a BH. We can see this by considering outgoing radial null geodesics:

$$r_{out} = a(\tau) \int_\tau^\infty \frac{d\tau}{a(\tau)} = a \int_a^\infty \frac{da}{a^2 H(a)} < \frac{1}{H_\Lambda} \equiv r_\Lambda \quad (15)$$

which shows that signals can not escape from the inside of  $r_\Lambda$ .

## 3 PROPER COORDINATES

The most general shape for a metric with spherical symmetry in proper or SW coordinates  $(t, r, \delta, \theta)$  is Padmanabhan (2010):

$$ds^2 = g_{\mu\nu} dx^\mu dx^\nu = -(1 + 2\Psi) dt^2 + \frac{dr^2}{1 + 2\Phi} + r^2 d\omega_k^2 \quad (16)$$

where  $d\omega_k$  was introduced in Eq.9 to allow for non-flat space.  $\Psi(t, r)$  and  $\Phi(t, r)$  are the two gravitational potentials. The Weyl potential  $\Phi_W$  is the geometric mean of the two:

$$(1 + 2\Phi_W)^2 = (1 + 2\Phi)(1 + 2\Psi) \quad (17)$$

$\Psi$  describes propagation of non-relativist particles and  $\Phi_W$  the propagation of light. For  $p = -\rho$  we have  $\Psi = \Phi = \Phi_W$ . Eq.16 can also be used to describe the BH.SW solution (or any other solution) as a perturbation ( $2|\Phi| < 1$ ) around a FLRW background:

$$ds^2 \simeq -(1 + 2\Psi) dt^2 + (1 - 2\Phi) a^2 d\chi^2 + a^2 \chi^2 d\omega_k^2 \quad (18)$$

where  $r = a(\tau)\chi$  and  $t \simeq \tau$ . The same result follows from perturbing the FLRW metric in Eq.9. EFE for Eq.16 are well known, e.g. see Eq.(7.51) in Padmanabhan (2010). For a static perfect fluid with arbitrary  $\rho(r)$  inside  $r_{SW}$  and empty space ( $\Lambda = 0$ ) outside, we have  $G_0^0 = -8\pi G \rho(r)$ . This can be solved using  $m(r) \equiv \int_0^r \rho(r) 4\pi r^2 dr$ :

$$\Phi(r) = -\frac{Gm(r)}{r} = \begin{cases} -GM/r & \text{for } \rho(r) = M \delta_D(r) \\ -\frac{1}{2}(r/r_0)^2 & \text{for } \rho(r) = \rho_0 \equiv \frac{3}{8\pi r_0^2} \end{cases} \quad (19)$$

$\Psi(r)$  depends on  $G_1^1$  and  $p(r)$ . For  $p = -\rho$  we have  $G_0^0 = G_1^1$  and the general solution with  $\Lambda \neq 0$  is:

$$\Phi = \Psi = -\frac{Gm(r)}{r} - \frac{\Lambda r^2}{6} \quad (20)$$

**Table 1.** Summary of metric notation used in this paper.

$-2\Phi(t, r)$	name	comment
$r_{SW}/r$	SW = Schwarzschild	BH.SW, outside BHU
$r^2/r_\Lambda^2$	dS = deSitter	static, inside BH.fv
$r_{SW}/r + r^2/r_\Lambda^2$	dSW = dS-SW	static, outside BHU
$r^2/r_H^2$	dSE = dS Extension	FLRW, inside BH.u

The remaining EFE,  $G_2^2 = G_3^3$  correspond to energy conservation  $\nabla_\mu T_\nu^\mu = 0$ . For a comoving observer  $u = 0$  in a perfect fluid of Eq.4:

$$\partial_t \rho = -\frac{\rho + p}{1 + 2\Phi} \partial_t \Phi; \quad \partial_r p = \frac{\rho + p}{1 + 2\Psi} \partial_r \Psi \quad (21)$$

Note how  $\rho = -p$  results in constant  $\rho$  and  $p$  everywhere, but with a discontinuity at  $2\Phi = 2\Psi = -1$ . This means that  $\rho$  and  $p$  can be constant, but different in both sides of  $2\Phi = 2\Psi = -1$ . This can be addressed with the study of junction conditions (see §4.3). We can also consider anisotropic pressure  $p_{\parallel} \neq p_{\perp}$  (Brustein & Medved 2019; Dymnikova 2019) which can result from non canonical scalar field (Díez-Tejedor & Feinstein 2006). Empty space ( $\rho = p = \rho_\Lambda = 0$ ) in Eq.20 results in the BH.SW metric:

$$2\Phi = 2\Psi = -2GM/r \equiv -r_{SW}/r \quad (22)$$

In the presence of  $\Lambda$ , this metric corresponds to  $\rho_\Lambda = V(\varphi) + \Lambda/8\pi G = 0$  in Eq.8. There is a trapped surface at  $r = r_{SW}$  ( $2\Phi = -1$ ). Outgoing radial null geodesics cannot leave the interior of  $r_{SW}$ , while incoming ones can cross inside. The solution to Eq.20 for  $\rho = p = M = 0$ , but  $\rho_\Lambda \neq 0$  results in deSitter (dS) metric:

$$2\Phi = 2\Psi = -r^2 H_\Lambda^2 \equiv -r^2/r_\Lambda^2 \quad (23)$$

where  $H_\Lambda^2 \equiv 8\pi G \rho_\Lambda/3$  and  $\rho_\Lambda = \Lambda/(8\pi G) + V(\varphi)$ . We can immediately see that this solution is the same as the interior of a BH with constant density in Eq.19 with  $\rho_0 = \rho_\Lambda$ . Topologically, dS metric corresponds to the surface of a hypersphere of radius  $r_\Lambda$  in a flat spacetime with an extra spatial dimension (see Appendix A). As in the BH.SW metric, dS metric also has a trapped surface at  $r = r_\Lambda$  ( $2\Phi = -1$ ). Radial null events ( $ds^2 = 0$ ) connecting  $(0, r_0)$  with  $(t, r)$  follow:

$$r = r_\Lambda \frac{r_\Lambda + r_0 - (r_\Lambda - r_0)e^{-2t/r_\Lambda}}{r_\Lambda + r_0 + (r_\Lambda - r_0)e^{-2t/r_\Lambda}} \quad (24)$$

so that it takes  $t = \infty$  to reach  $r = r_\Lambda$  from any point inside. The BH.SW metric is singular at  $r = 0$ , while dS is singular at  $r = \infty$ . In comoving coordinates, dS singularity corresponds to a comoving Hubble horizon that shrinks to zero (see Fig.4). But note that this singularity can not be reached from the inside because of the trapped surface at  $r_\Lambda$  in Eq.24. The inside observer is trapped, also like in the FLRW case. In fact, both metrics are equivalent for  $H = H_\Lambda$  (see Mitra 2012) which explains why the dS metric reproduces primordial inflation in comoving coordinates.

As first noticed by Einstein (O’Raifeartaigh & Mitton 2015), the Steady-State Cosmology (SSC), with a perfect cosmological principle, is also reproduced by dS metric. But contrary to the original SSC proposal of Bondi & Gold (1948); Hoyle (1948), there is no need for continuous matter creation (or a C-field) because the metric is expanding in comoving coordinates but is static in proper coordinates because  $\rho_\Lambda = V(\varphi)$  is trapped to a fixed FV value in Eq.8.

We will also consider a generalization of dS metric, which we call dS extension (dSE), which is just a recast of the general case:

$$2\Phi(t, r) \equiv -r^2 H^2(t, r) \equiv -r^2/r_H^2 \quad (25)$$

where  $r_H \equiv 1/H$  corresponds to the Hubble radius. Table 1 shows

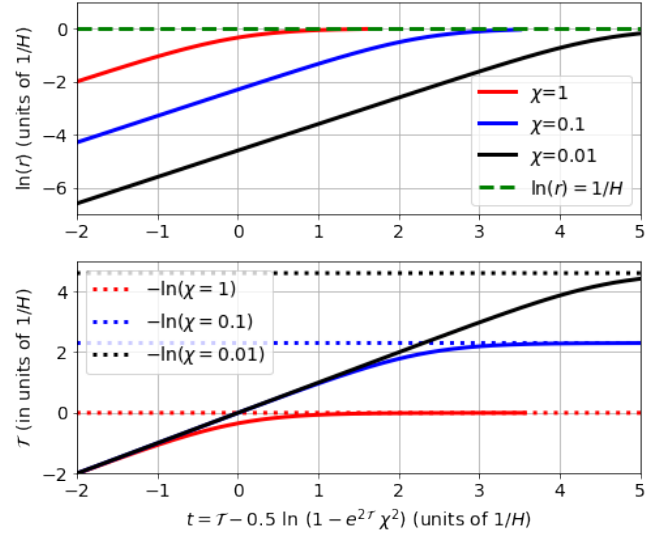


**Figure 2.** Logarithm of proper radius  $r = a(\tau)\chi$  (top) and comoving time  $\tau$  (bottom) as a function of SW time  $t$  in Eq.29 for  $a(\tau) = e^{\tau H_\Lambda}$  and different values of  $\chi$ . All quantities are in units of  $1/H_\Lambda$ . For early time or small  $\chi$ :  $\tau \approx t$ . A fix  $\chi$  acts like an Horizon: as  $t \rightarrow \infty$  we have  $\tau \rightarrow -\ln \chi$  (dotted), which freezes inflation to:  $r = a\chi \Rightarrow e^{-\ln(H_\Lambda \chi)} \chi = 1/H_\Lambda$  (dashed).

a summary of metrics considered in this paper. When we have both  $M$  and  $\rho_\Lambda$  constant, the solution to Eq.20 is:  $2\Phi = 2\Psi = -r^2 H_\Lambda^2 - r_{SW}/r$ , which corresponds to dS-SW (dSW) metric, a BH.SW within a dS background. Solution of a BH inside a FLRW metric also exist (e.g see Kaloper et al. 2010). Here we will show that GR solutions also exist for a FLRW inside a BH (or inside a larger FLRW metric).

### 3.1 The FLRW metric in proper coordinates

Consider a change of variables from  $x^\mu = [t, r]$  to comoving coordinates  $\xi^\nu = [\tau, \chi]$ , where  $r = a(\tau)\chi$  and angular variables  $(\delta, \theta)$  remain the same. The metric  $g_{\mu\nu}$  in Eq.16 transforms to  $f_{\alpha\beta} = \Lambda_\alpha^\mu \Lambda_\beta^\nu g_{\mu\nu}$ , with  $\Lambda_\nu^\mu \equiv \frac{\partial x^\mu}{\partial \xi^\nu}$ . If we use:

$$\Lambda = \begin{pmatrix} \partial_\tau t & \partial_\chi t \\ \partial_\tau r & \partial_\chi r \end{pmatrix} = \begin{pmatrix} (1 + 2\Phi_W)^{-1} & arH(1 + 2\Phi_W)^{-1} \\ rH & a \end{pmatrix}, \quad (26)$$

with  $2\Phi = -r^2 H^2$  and arbitrary  $a(\tau)$  and  $\Psi$ :

$$f_{\alpha\beta} = \Lambda^T \begin{pmatrix} -(1 + 2\Psi) & 0 \\ 0 & (1 + 2\Phi)^{-1} \end{pmatrix} \Lambda = \begin{pmatrix} -1 & 0 \\ 0 & a^2 \end{pmatrix}, \quad (27)$$

In other words, these two metrics are the same:

$$-(1 + 2\Psi)dt^2 + \frac{dr^2}{1 - r^2 H^2} + r^2 d\omega_k^2 = -d\tau^2 + a^2 \left[ d\chi^2 + \chi^2 d\omega_k^2 \right] \quad (28)$$

dSE metric of Eq.25 corresponds to the FLRW metric with  $H(t, r) = H(\tau)$ : this is a hypersphere of radius  $r_H$  that tends to  $r_\Lambda$  (see Appendix A). This frame duality can be understood as a Lorentz contraction  $\gamma = 1/\sqrt{1 - v^2}$  where  $v = Hr$ . The SW frame, that is not moving with the fluid, sees a moving fluid element  $ad\chi$  contracted by the Lorentz factor  $\gamma$ :  $ad\chi \Rightarrow \gamma dr$ . For constant  $H$ , the FLRW metric corresponds the interior of a BH with constant density in Eq.19. In general, we can find  $\Psi = \Psi(t, r)$  and  $t = t(\tau, \chi)$  or  $\tau = \tau(t, r)$  given  $a(\tau)$ . For  $a(\tau) = e^{\tau H_\Lambda}$  we have  $2\Psi = 2\Phi = -r^2 H^2$  and

$$t = t(\tau, \chi) = \tau - \frac{1}{2H_\Lambda} \ln [1 - H_\Lambda^2 a^2 \chi^2], \quad (29)$$



where  $r < r_\Lambda = 1/H_\Lambda$ , which reproduces dS metric. In comoving coordinates the metric is inflating exponentially:  $a = e^{\tau H_\Lambda}$ , while in proper coordinates it is static. Fig.2 illustrates how this is possible and shows how  $\tau = \tau(t, r)$  freezes (see Mitra 2012 for some additional discussion). The general frame duality of Eq.28, from a comoving frame to a proper SW frame, is a new result as far as we know, and a key ingredient to interpret our new physical BH solution.

## 4 BLACK HOLE SOLUTIONS

### 4.1 False Vacuum Black Hole (BH.fv) solution

Eq.22 and Eq.23 are the simplest solutions to EFE. They correspond to some form of empty space. The simplest modeling of physical BH interior is a combination of the two (see Eq.2.2 in Blau et al. 1987):

$$\rho = -p = \begin{cases} 0 & \text{for } r > r_{SW} \\ \Delta & \text{for } r < r_{SW} \end{cases} \quad (30)$$

where  $\Delta > 0$ . To recover the BH.SW solution outside, we use  $V_0 = \Lambda_{\text{out}} = 0$ . In a more realistic situation, on larger scales the BH.SW metric should be considered a perturbation of FLRW background, e.g. Eq.18, with  $\Lambda_{\text{out}} \neq 0$  and  $V_0 \neq 0$ , in fact we could also have a FLRW metric outside (see Appendix B). The solution to EFE in Eq.20 for Eq.30 (which we called BH.fv) is then:

$$2\Phi = 2\Psi = \begin{cases} -r_{SW}/r & \text{for } r > r_{SW} \equiv 2GM \\ -r^2 H_{\Lambda_{\text{in}}}^2 & \text{for } r < r_{SW} = r_{\Lambda_{\text{in}}} \equiv 1/H_{\Lambda_{\text{in}}} \end{cases} \quad (31)$$

where:  $\rho_{\Lambda_{\text{in}}} = \rho_{BH} = \Delta$  and  $M = \frac{4\pi}{3} r_{SW}^3 \Delta$ . Recall that  $\Lambda = V_0 = 0$  and  $\rho_{\Lambda_{\text{in}}}$  refers to the effective  $\Lambda$  density inside the BH. The above solution has no singularity at  $r = 0$ . Note how, contrary to what happens in the BH.SW, in the BH.fv solution, the metric components don't change signature as we cross inside  $r_{SW}$ . In both sides of  $r_{SW}$  we have constant but different values of  $p$  and  $\rho$ . This comes from energy conservation in Eq.21. There is a discontinuity at  $2\Phi = -1$  where  $r = r_{SW}$ , in agreement with Eq.21, but the metric is static and continuous at  $r_{SW}$ . This solution only happens when  $r_{SW} = r_{\Lambda_{\text{in}}} = (8\pi G \Delta / 3)^{-1/2}$ . The smaller  $\Delta$  the larger and more massive the BH. In the limit  $\Delta \Rightarrow 0$ , we have  $r_{SW} = r_{\Lambda_{\text{in}}} \Rightarrow \infty$  and we recover Minkowski space, as expected.

At a fixed location, the scalar field  $\varphi$  inside the BH is trapped in a stable configuration ( $\rho = V_0 + \Delta$ ) and can not evolve ( $K = 0$  in Eq.7). The same happens for the field outside (see Fig.1). A FV in Eq.30 with equal  $\Delta$  but with smaller initial radius  $r = R < r_{SW}$  is subject to a pressure discontinuity at  $r = R$  which is not balanced in Eq.21 and results in a bubble growth (Blau et al. 1987; Aguirre & Johnson 2005). Such boundary grows and asymptotically reaches  $R = r_{SW}$  (see top panel of Fig.2, Fig.3 and Eq.42). The inside of  $r_{SW}$  is causally disconnected, so the pressure discontinuity does not act on  $r = r_{SW}$ , which corresponds to a trapped surface.

### 4.2 Black Hole Universe (BH.u) solution

We next look for solutions where we have matter  $\rho_m = \rho_m(t, r)$  and radiation  $\rho_R = \rho_R(t, r)$  inside but an empty BH.SW outside:

$$\rho(t, r) = \begin{cases} -p = 0 & \text{for } r > r_{SW} \\ \Delta + \rho_m + \rho_R & \text{for } r < r_{SW} \end{cases} \quad (32)$$

Note that  $p = -\Delta + \rho_R/3 \neq -\rho$  inside, so that  $\partial_t \Phi \neq 0$  and  $u \neq 0$ : the fluid inside has to move relative to SW frame of the outside observer.

For  $r > r_{SW}$ , the solution is the same as Eq.31. For the interior we use the dSE notation in Eq.25:  $2\Phi(t, r) \equiv -r^2 H^2(t, r)$ , so that:

$$2\Phi(t, r) = \begin{cases} -r_{SW}/r & \text{for } r > r_{SW} = 2GM \\ -r^2 H^2(t, r) & \text{for } r < r_{SW} = 1/H_{\Lambda_{\text{in}}} \end{cases} \quad (33)$$

where  $r_{SW} = 2GM = 1/H_{\Lambda_{\text{in}}}$  as before. We can find the interior solution with a change of variables of Eq.26-28. This converts dSE metric into FLRW metric so the solution is just  $H(t, r) = H(\tau)$ . Given  $\rho$  and  $p$  in the interior of a BH we can use Eq.12 with  $\rho_{\Lambda_{\text{in}}} = \Delta = 3r_{SW}^{-2}/8\pi G$  to find  $H(\tau)$  and  $a(\tau)$ . We call this a BH universe (BH.u). To complete the solution, i.e. to find  $\Psi$  and  $\tau = \tau(t, r)$ , we need to solve Eq.26 with  $2\Phi = -r^2 H^2(\tau)$ . For  $H(\tau) = H_{\Lambda_{\text{in}}}$  the solution is  $\Psi = \Phi$  and Eq.29. The flat FLRW metric with  $H = H_{\Lambda_{\text{in}}}$  becomes dS metric in Eq.23 as in the BH.fv solution.

Given  $T_{\mu\nu}$  in Eq.10 we can find  $\tilde{T}_{\alpha\beta}$  in the proper frame using the inverse matrix of Eq.26:  $\tilde{T}_{\alpha\beta} = (\Lambda^{-1})_\alpha^\mu (\Lambda^{-1})_\beta^\nu T_{\mu\nu}$ :

$$\tilde{T}_0^0 = -\frac{\rho - p 2\Phi}{1 + 2\Phi} ; \tilde{T}_1^1 = \frac{p - \rho 2\Phi}{1 + 2\Phi} \quad (34)$$

which is independent of  $\Psi$ . Comparing to Eq.4 gives the velocity in the proper frame  $u^2 = -2\Phi = r^2 H^2$ , which is just the Hubble law. The Lorentz factor is  $\gamma = (1 + 2\Phi)^{-1/2}$  so that  $\gamma dr$  gives the proper length, in agreement with Eq.16.

Solution  $H(t, r) = H(\tau)$  in Eq.33 is valid for all  $r < r_{SW} = 1/H_{\Lambda_{\text{in}}}$  because  $H(\tau) > H_{\Lambda_{\text{in}}}$ . We can see this by considering outgoing radial null geodesic in the FLRW metric of Eq.15. which shows that signals can not escape from the inside to the outside of the BH.u. But incoming radial null geodesics  $a(\tau) \int_0^\tau \frac{d\tau}{a(\tau)}$  can in fact be larger than  $r_{SW}$  if we look back in time. This shows that inside observers are trapped inside the BH.u but they can nevertheless observe what happened outside (Gaztañaga & Fosalba 2021).

### 4.3 Junction conditions

We can arrive at the same BHU (BH.fv and BH.u) solutions using the junction conditions of Israel (1967). Here we follow closely the notation in §12.5 of Padmanabhan (2010). We will combine two solutions to EFE with different energy content, as in Eq.32, on two sides of a timelike hypersurface  $\Sigma = \mathcal{M}_{\text{in}} \cap \mathcal{M}_{\text{out}}$ . The inside  $g_{\text{in}}$  is FLRW metric (or dS metric for  $H = H_{\Lambda_{\text{in}}}$ ) and the outside  $g_{\text{out}}$  is BH.SW metric. This is similar to the case §12.5.1 in Padmanabhan (2010) with the difference that we use  $k = 0$  (instead of  $k = 1$ ) and consider a general FLRW solution  $a(\tau)$  with  $\Lambda$ ,  $\rho_m$  and  $\rho_R$  (instead of a pressure-free dust model without  $\Lambda$ ). This is relevant to provide the limiting trapped surface  $r_{SW} = \sqrt{3/\Lambda}$ . We define  $\Sigma$  to be fixed in comoving coordinates at  $\chi = r_{SW}$ , so  $\Sigma$  only depends  $\tau$  (here we fix  $a = 1$  when  $\chi = r_{SW}$ ). For the outside SW coordinate system,  $\Sigma_{\text{out}}$  is described by  $r = R(\tau)$  and  $t = T(\tau)$ , where  $\tau$  is the comoving time in the FLRW metric. We then have:

$$dr = \dot{R} d\tau ; dt = \dot{T} d\tau, \quad (35)$$

where the dot refers to derivatives with respect to  $\tau$ . The induced metric  $h_{\text{in}}$  on the inside of  $\Sigma_{\text{in}}$  with  $y^a = (\tau, \delta, \theta)$  and fixed  $\chi = r_{SW}$ , is:

$$ds_{\Sigma}^2 = h_{ab} dy^a dy^b = -d\tau^2 + a^2(\tau) r_{SW}^2 d\omega^2 \quad (36)$$

has to agree with  $h_{\text{out}}$ , the BH.SW metric outside at  $\Sigma_{\text{out}}$ :

$$-F dt^2 + F^{-1} dr^2 + r^2 d\omega^2 = -(F\dot{T}^2 - \dot{R}^2/F) d\tau^2 + R^2 d\omega^2 \quad (37)$$

where  $F = 1 - \frac{r_{SW}^2}{R^2}$ . The matching condition  $h_{\text{in}} = h_{\text{out}}$  is:

$$R(\tau) = a(\tau) r_{SW} ; F\dot{T} = \sqrt{\dot{R}^2 + F} \equiv \beta(R, \dot{R}) \quad (38)$$

Thus, for a given FLRW solution  $a(\tau)$  we know both  $R$  and  $\beta$ . The extrinsic curvature  $K_{in/out}$  normal to  $\Sigma_{in/out}$  from each side is:

$$\begin{aligned} K_{in\tau}^\tau &= 0 \quad ; \quad K_{in\theta}^\theta = K_{in\delta}^\delta = -\frac{1}{ar_{SW}} \\ K_{out\tau}^\tau &= \frac{\dot{\beta}}{R} \quad ; \quad K_{out\theta}^\theta = K_{out\delta}^\delta = -\frac{\beta}{R} \end{aligned} \quad (39)$$

Thus, the second matching condition  $K_{in} = K_{out}$  requires  $\beta = 1$ , which using Eq.38 results in:

$$\begin{aligned} \dot{R}^2 &= R^2 H^2 = \frac{r_{SW}}{R} \quad (40) \\ \dot{T} &= \frac{1}{1-R^2 H^2} \Rightarrow T = \int \frac{dR}{HR(1-H^2 R^2)} \quad (41) \end{aligned}$$

This results in  $2\Psi = 2\Phi = -H^2 R^2 = -r_{SW}/R$  in the junction  $\Sigma$  as in Eq.33. This is the dSE generalization of dS space for arbitrary  $a(\tau)$ :  $2\Psi = 2\Phi = -R^2/r_H^2$  with  $r_H \equiv 1/H(\tau)$  in Eq.25. The critical density inside  $r_H$ , corresponds to that of a BH: from Eq.40 we have  $H^2 = r_{SW}/R^3 = 8\pi G\rho/3$ .

This  $\Sigma$  junction grows and tends to  $r_{SW} = 1/H_{\Lambda_{in}}$ . It takes  $T = \infty$  in the SW time of Eq.41 to asymptotically reach  $r_{SW} = 1/H_{\Lambda_{in}}$  (see Fig.2). In this limit, Eq.40 reproduces the BH.fv junction of Eq.31 for constant  $H = H_{\Lambda_{in}}$ . Before that, the BHU junction is not static (not even in the SW frame) as  $H$  decays into  $H_{\Lambda_{in}}$  when  $R$  grows to  $r_{SW}$ . Despite the discontinuity in  $\rho$  at  $r_{SW}$ , the BHU metric and extrinsic curvature are continuous when we join them with the expanding timelike hypersurface of  $\Sigma$ . This proves that the BHU metric is also a solution to EFE and there are no surface terms in the junction (see Eq.21.167 in Misner et al. 1973). This does not require that the metrics have identical Riemann tensor or invariant scalars.

The effective  $\Lambda$  term corresponds to a trapped surface  $r_{SW} = 1/H_{\Lambda_{in}}$  in the FLRW (or dS) metric which matches the horizon of a BH in empty space (see Fig.5). In a more realistic case, the external background is not empty and we then need to study the junction of two FLRW with two different effective  $\Lambda_{in}$  and  $\Lambda_{out}$ , matter content and Hubble laws  $a(\tau)$ . The effective  $\Lambda_{in}$  will be the trapped surface of a BH inside the outside FLRW metric (see also Appendix B). Here we just want to point out that such solutions exist and more work is needed to workout more realistic situations.

This junction solution is similar to the one found for Bubble Universes (e.g. see Blau et al. 1987; Aguirre & Johnson 2005 and references therein) but with some important differences. Our solution is more general as it corresponds to the FLRW metric (which includes matter and radiation as well as a FV), which is not static in the SW frame. The Bubble Universes instead only use dS metric in its static representation. Also, a surface term with  $\sigma \neq 0$  is needed to match the resulting discontinuity in the  $K$  curvature. The BHU junction is continuous in comoving coordinates and has no surface terms.

#### 4.4 Evolving junction: internal BH dynamics

The junction conditions indicate that the division between interior and exterior solutions in Eq.31 and Eq.33 is not  $r_{SW}$ , which is only the limiting case. This is illustrated in Fig.3. That both the metric and the external curvature are continuous at  $R$  shows that there are no surface terms and the join metric is a solution to EFE (see Eq.21.167 in Misner et al. 1973). The energy-momentum tensor  $T_{\mu\nu}$  corresponding to this solution has a discontinuity (as expected for a BH):  $\rho_{\Lambda_{in}} = -p_{\Lambda_{in}} \neq 0$  for  $r < R$  and  $\rho_{\Lambda_{out}} = 0$  for  $r > R$ .

Inside the physical BH we have an expanding junction:  $r = R(\tau) = a(\tau)r_{SW}$ . Because  $R(\tau) < r_{SW}$  is always inside  $r_{SW}$ , the external SW observer can not distinguish this evolving junction from the

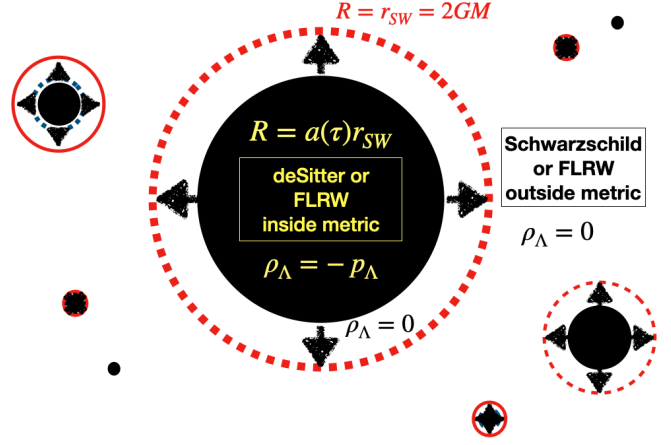


**Figure 3.** Illustration of the interior dynamics of a BHU. The junction  $R = a(\tau)r_{SW}$  (black disk) grows towards the SW radius  $R = r_{SW}$  (dashed red circle). The inside of  $R = a(\tau)r_{SW}$  is dS or a FLRW metric (dominated by negative pressure:  $\rho = -p$ ) while the outside is empty BH.SW metric, a perturbation around a FLRW background with other BHs and matter.

limiting static one  $r = r_{SW}$ . This is why we chose to express the solution this way. The junction  $R(\tau)$  grows and asymptotically tends to  $r_{SW}$  as shown in Fig.3. This happens at a finite comoving time  $\tau_{\Lambda_{in}}$  as in the top panel of Fig.2. The exact function depends on the form of  $a = a(\tau)$ . For constant  $\dot{a}/a = H = H_{\Lambda_{in}} = 1/r_{SW}$ , the solution can be expressed analytically as:

$$R(\tau) = R_0 e^{H_{\Lambda_{in}} \tau} = e^{H_{\Lambda_{in}} (\tau - \tau_{\Lambda_{in}})} r_{SW} \quad (42)$$

where we have chosen  $a = 1$  when  $R = r_{SW}$ . We start with a finite size  $R = R_0 = a_0 r_{SW}$  at  $\tau = 0$ , where  $a_0 = e^{-\tau_{\Lambda_{in}} H_{\Lambda_{in}}}$ . After  $\tau_{\Lambda_{in}} H_{\Lambda_{in}}$  e-folds,  $R_0$  grows into  $R = r_{SW}$ . This inflation stops asymptotically at  $\tau = \tau_{\Lambda_{in}} = -r_{SW} \ln a_0$ . We can think of  $R_0$  as a quantum size (FV) fluctuation of energy  $\rho_{\Lambda_{in}} = \Delta$ , which (in empty space) will inflate to size  $r_{SW} = 1/H_{\Lambda_{in}} = (8\pi G\Delta/3)^{-1/2}$ .

This new solution to EFE is not just an arbitrary matching of two other random solutions. It is a new solution of a new physical configuration given by the energy content in Eq.32. This configuration corresponds exactly to our definition of a generic physical BH. The one we set to find in the introduction and whose horizon separates two regions with different matter-energy content. The same horizon defines the junction of two well known solutions to EFE.

## 5 IMPLICATIONS FOR OUR UNIVERSE

The BH.fv interior, dS metric, can be transformed into a FLRW metric with constant  $H = H_{\Lambda_{in}}$ . This frame duality provides a new interpretation for the BH.fv solution in Eq.31. This is not only a solution for a BH inside a universe. The inside comoving observer, sees this solution as an expanding inflationary universe inside a BH, even when the metric is static in proper coordinates and  $r = r_{SW}$  is fixed. The same happens with the BH.u solution of Eq.33, which is equivalent to a child FLRW in the interior.

Recall how the outside BH.SW solution should be considered a perturbation of a parent FLRW in Eq.18. So we have two nested FLRW metrics which are connected with the BHU. Each one could have a different effective  $\rho_{\Lambda}$  (or FV). So could our universe be a child FLRW metric? The fact that we have measured  $\rho_{\Lambda} \neq 0$  provides a

strong indication that this is the case. It is hard to explain what  $\Lambda$  means or the coincidence problem otherwise (see below).

The change of variables in Eq.26 is only valid for proper coordinates that are centered at the center of the BH location. But in the transformed (comoving) frame of Eq.28 any point inside is subject to the same expansion law with equal  $a(\tau)$ . From every point inside de BHU, comoving observers will see an homogeneous and isotropic space-time around them (see bottom left of Fig.5). At least all the way back in time to  $r_{SW} = 1/H_\Lambda$ , which is in their distant past. All points inside the BH were at the center in their distance past (just as in the homogeneous expanding universe). Even if all points inside see an homogeneous expansion, as they look back in time from a position that is off centered, some regions of the sky will be closer to the past horizon than others. This could result in some significant deviations from isotropy and homogeneity on the largest scales. Regions outside the trapped surface could have a similar background but with uncorrelated fluctuations that fit different parameters. Such deviations have already been measured in the form of large scale CMB anomalies and variations of cosmological parameters (see Fosalba & Gaztañaga 2021).

Note how we can have FVs inside other FVs (see Fig.1). So we can have BHs inside other BHs or FLRW metrics inside other FLRW universes. Mathematically this looks like a Matryoshka (or nesting) doll or a fractal structure. But physically, in the common SW frame, each BH has a different mass and therefore different physical properties. The child FLRW BHU have smaller mass (and larger FV) than the parent BHU. A BHU of one solar mass can have a FLRW metric inside but this inside will not have any galaxies and is going to be very different from that in a  $M \approx 5.8 \times 10^{22} M_\odot$  BHU, like ours, which contains billions of galaxies and BHs of many different sizes. So each BHU layer could be physically quite different from the next, unlike Matryoshka dolls or fractal structures.

### 5.1 The evolution of the BH universe

How did the universe evolve into the solution of Eq.33? This is an important question. It is not enough to find a solution to EFE. We need to make sure that such a configuration can be achieved in a causal way. Without  $\Lambda$ , the FLRW universe has no causal origin: the Hubble rate (in Eq.12) is the same everywhere, not matter how far, and this is not causally possible. The comoving coordinate  $\chi = r_{SW}$  that fixes the junction in §4.3 above can be identified as the causal horizon  $\chi_\S$  in the zero action principle (Gaztañaga 2021). In the FLRW Universe, the Hubble Horizon  $r_H$  is defined as  $r_H = c/H$ . Scales larger than  $r_H$  cannot evolve because the time a perturbation takes to travel that distance is larger than the expansion time. This means that  $r > r_H$  scales are "frozen out" (structure can not evolve) and are causally disconnected from the rest. Thus,  $c/H$  represents a dynamical causal horizon that is evolving.

The standard evolution of our universe is shown in Fig.4. Note that here we choose  $a = 1$  now, as opposed to Fig.3 where  $a = 1$  corresponds to  $R = r_{SW}$ . It turns out that both are not so different (the so call coincidence problem in cosmology). A primordial field  $\varphi$  settles or fluctuates into a false (or slow rolling) vacuum which will create a BH.fv with a junction  $\Sigma$  in Eq.36, where the causal boundary is fixed in comoving coordinates and corresponds to the particle horizon during inflation  $\chi_\S = c/(a_i H_i)$  or the Hubble horizon when inflation begins. The size  $R = a(\tau)\chi_\S$  of this vacuum grows and asymptotically tends to  $r_H = c/H$  following Eq.40 with  $H = H_i$ . The inside of this BH will be expanding exponentially  $a = e^{\tau H_i}$  while the Hubble horizon is fixed  $1/H_i$ . According to standard models of primordial inflation (Starobinskiĭ 1979; Guth 1981;

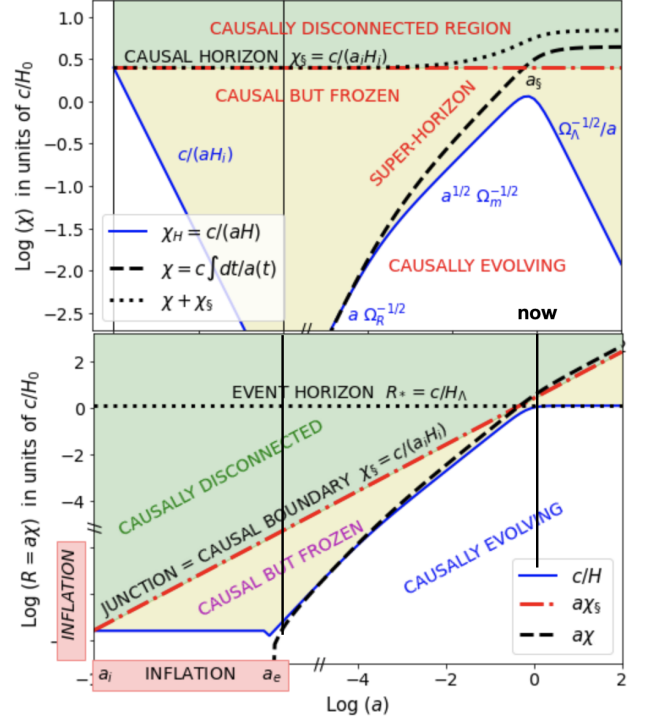


**Figure 4.** Comoving (top)  $\chi$  and proper (bottom)  $R = a(\tau)\chi$  radial coordinate in units of  $c/H_0$  as a function of cosmic time  $a$  (scale factor). The Hubble horizon  $c/H$  (blue continuous line), is compared to the observable universe  $\chi$  after inflation (dashed line) and the primordial causal boundary  $\chi_\S = c/(a_i H_i)$  (dot-dashed red line). Larger scales (green shading) are causally disconnected, smaller scales (yellow shading) are dynamically frozen. After inflation  $c/H$  grows again. At  $a \approx 1$  (close to now) the Hubble horizon reaches our event horizon  $r_{SW} = c/H_\Lambda$ .

Linde 1982; Albrecht & Steinhardt 1982), this inflation ends and vacuum energy excess converts into matter and radiation (reheating). This results in BH.u, where the infinitesimal Hubble horizon starts to grow following the standard BB evolution.

Note that the inflation in the BH.fv solution (i.e. Eq.42) stops naturally at cosmic time  $\tau_i = -H_i^{-1} \ln \chi_\S H_i$  (see Fig.2) when proper distance is  $r = a(\tau)\chi_\S = 1/H_i$ . In standard models of primordial inflation,  $H_i$  is much larger than  $H_\Lambda$  so that  $1/H_i$  is much smaller than  $1/H_\Lambda$ . So a quantum FV fluctuation  $\Delta$  only grows to a maximum size  $R = r_{SW} = (8\pi G \Delta^2)^{-1/2} = 1/H_i$ . Something else has to happen if we want the size to become cosmological. It could be reheating or some other mechanism. Quantum tunneling into smaller  $\Delta$  (see Fig.1) also produces larger  $r_{SW}$ . Matter and radiation can also appear some other ways: from the original quantum fluctuations, from quantum tunneling to/from other FV, from infall of matter from outside (see §2.1-6.3) or from Hubble damping of smaller FV that turn into BHs (see §2.1). Regardless of these formation details,  $\chi_\S$  remains the causal scale for the original BH.fv inflation in Eq.42. Recall that the BH.fv solution requires a discontinuity in  $\rho_\Lambda = 0$ , so this BH.fv evolution happens with independence of what we assume about  $\Lambda$  in EFE. A causal boundary in empty space generates a boundary term in the action that fixes the value of  $\Lambda$  to  $\Lambda = 4\pi G < \rho + 3p >$ , where the average is over the light-cone inside  $\chi_\S$  (Gaztañaga 2021). This  $\Lambda$  represents a trapped surface for the emerging BH.u universe.



The observable universe (or particle horizon) after inflation is:

$$\chi_O = \chi_O(a) = \int_{a_e}^a \frac{d \ln a'}{a' H(a')} = \chi_O(1) - \bar{\chi}(a), \quad (43)$$

where  $a_e$  is the scale factor when inflation ends. For  $\Omega_\Lambda \simeq 0.7$ , the particle horizon today is  $\chi_O(1) \simeq 3.26c/H_0$  and  $\bar{\chi}(a) = \int_a^1 d \ln a' / (a'H)$  is the radial lookback time, which for a flat universe agrees with the comoving angular diameter distance,  $d_A = \bar{\chi}$ . The observable universe becomes larger than  $r_{SW} = r_\Lambda$  when  $a > 1$ , as shown in Fig.4 (compare dotted and dashed lines). This shows that, observers like us, living in the interior of the BH universe, are trapped inside  $r_{SW}$  but can nevertheless observe what happened outside. We can estimate  $\chi_\S$  from  $\rho_\Lambda = \langle \rho_m/2 + \rho_R \rangle$ , where the average is in the lightcone inside  $\chi_\S$ . For  $\Omega_\Lambda \simeq 0.7$  Gaztañaga (2021) found:  $\chi_\S \simeq 3.34c/H_0$  which is close to  $\chi_O$  today. But imagine that  $\Omega_\Lambda$  is caused by some DE component and has nothing to do with  $\chi_\S$ . We still have that  $\chi_\S \lesssim \chi_O$ , because otherwise  $\chi_\S$  would have crossed  $RH = 1$  early on, resulting in smaller  $\chi_O$  than measured (see Fig.4).

Thus, at the time of CMB last scattering (when  $d_A \simeq \chi_O$ ),  $\chi_\S$  corresponds to an angle  $\theta = \chi_\S/d_A \lesssim 1$  rad  $\simeq 60$  deg. So we can actually observe scales larger than  $\chi_\S$ . Scales that are not causally connected! This could be related to the so-called CMB anomalies (i.e. apparent deviations with respect to simple predictions from  $\Lambda$ CDM, see Gaztañaga 2021; Fosalba & Gaztañaga 2021 and references therein), or the apparent tensions in measurements from vastly different cosmic scales or times (e.g. Planck Collaboration 2020).

## 6 DISCUSSION & CONCLUSION

The SW metric in Eq.22 is well known and studied but the interior solution is not physical because it corresponds to a singular point source of mass  $M$  at  $r = 0$ . We have looked for classical non-singular GR solutions for a BH interior. Our motivation is to find a physical model and study if this results in some different properties for BHs. The outside manifold  $\mathcal{M}_{\text{out}}$  of a BH is approximated as empty space so the solution  $g_{\text{out}}$  is the BH.SW metric. Because the inside  $\mathcal{M}_{\text{in}}$  is causally disconnected,  $\mathcal{M}_{\text{out}}$  acts like a simple boundary condition. Given some  $\rho$  and  $p$  inside  $r_{SW}$ , we have solve EFE inside with such boundary condition to find  $g_{\text{in}}$ , the inside metric of a physical BH. To our surprise we have found that  $g_{\text{in}}$  is just the well known FLRW, the same metric that describes our universe! This frame duality, represented by Eq.26, has several observational consequences, as we will discuss below.

To impose the boundary at  $r_{SW}$  we have use the same (proper) SW coordinate frame that is not moving with the fluid so that  $T_0^1 \neq 0$ . This results in a solution for  $\mathcal{M}_{\text{in}}$  that is not static. We have verified Israel (1967) conditions to double check that the join manifold  $\mathcal{M}_{\text{in}} \cup \mathcal{M}_{\text{out}}$  is also a solution to EFE and there are no surface terms (see §4.3). This is different from just matching two random metrics. We can add both matter and radiation to both sides of  $r_{SW}$  and we still have a BHU solution. The BHU connects two FLRW metrics (see Fig.5) connected with BH.SW and an effective  $\Lambda$  term.

The relativistic version of Poisson equation comes from the geodesic deviation equation (see Eq.12 in Gaztañaga 2021):

$$\nabla_\mu \mathbf{g}^\mu = \frac{d\Theta}{ds} + \frac{1}{3}\Theta^2 = R_{\mu\nu} u^\mu u^\nu = \Lambda - 4\pi G(\rho + 3p) \quad (44)$$

where  $\mathbf{g}^\mu$  is the geodesic acceleration (Padmanabhan 2010). This is also the Raychaudhuri equation for a shear free, non rotating fluid where  $\Theta = \nabla_\nu u^\nu$  and  $s$  is proper time. The above equation is purely geometric: it describes the evolution in proper time of the dilatation

coefficient  $\Theta$  of a bundle of nearby geodesics. Note how  $\rho_\Lambda > 0$  produces acceleration and therefore expansion. A key point to the BHU solution is the  $\rho_\Lambda$  discontinuity at  $r = r_{SW}$  which could also be understood as a boundary to the Einstein-Hilbert action. The action on shell  $S^{\text{on-sh}}$  is a boundary term (Gaztañaga 2021):

$$S^{\text{on-sh}} = \int_M \frac{dM}{8\pi G} \nabla_\mu \mathbf{g}^\mu = \oint_{\partial M} \frac{dV_\mu \mathbf{g}^\mu}{8\pi G} \quad (45)$$

which is zero outside causal contact. This translates into Eq.C1 which addresses the coincidence problem (see Appendix C).

### 6.1 False Vacuum BH solution (BH.fv)

BH.fv corresponds to constant FV discontinuity (Eq.30) with dS metric inside (Eq.31), with a trapped surface which matches the BH.SW event horizon. A constant density (or negative pressure) corresponds to a centrifugal force,  $2\Phi = -(r/r_{SW})^2$  that opposes Newtonian gravity,  $2\Phi = -r_{SW}/r$ , i.e. Eq.20. The equilibrium happens when both forces are equal, which fixes  $r = r_{SW}$ , and correspond to stable circular Kepler orbits.

This solution is similar to the classical Bubble Universe solution (Blau et al. 1987; Frolov et al. 1989; Aguirre & Johnson 2005; Garriga et al. 2016; Kusenko 2020) including the gravastar (Mazur & Mottola 2015) and other extensions (e.g. Easson & Brandenberger 2001; Daghighi et al. 2000; Firouzjahi 2016; Oshita & Yokoyama 2018; Dymnikova 2019). But there are some important differences. In §4.3 we show that there are no surface terms so there is no need to introduce an additional term or surface tension ( $\sigma \neq 0$ ) in the bubble junction,  $\Sigma$ , to glue the BH.SW and dS metrics. We find that a timelike hypersurface, fix in comoving coordinates, provides a continuous solution. As far as we know, this is new (see also Stuckey 1994) and different from anisotropic models with negative radial pressure (Brustein & Medved 2019; Dymnikova 2019) or the above Bubble Universes, which have  $\sigma \neq 0$  over a spacelike or null bubble hypersurface.

### 6.2 The BH universe solution (BH.u)

In Eq.33 the BH interior is the FLRW metric. This BH.u solution is new, as far as we know. As discuss in the introduction, previous proposals were not proper or complete solutions within GR. We can have other BHs, matter and radiation inside a BHU within a larger space-time. The inside needs to be expanding as in the FLRW metric of Eq.9, with a trapped surface given by  $\rho_\Lambda$ . This holds the expansion and balance gravity at  $r_{SW}$  as in the BH.fv solution. The join FLRW+SW solution (Eq.33) is also a solution to Einstein's field equations as the two metrics reduce to the same form on a junction of constant  $\chi = r_{SW}$  in Eq.36, and the extrinsic curvature in Eq.39 is the same in both sides. The junction  $R(\tau)$  between interior and exterior solutions in Eq.31 and Eq.33 is not necessarily  $r_{SW}$ , which is the limiting case. The junction  $R(\tau)$  asymptotically tends to  $r_{SW}$  as shown in Fig.3.

The exterior metric could also be FLRW, as the BH.SW metric can be considered a local perturbation within a larger FLRW background with arbitrary  $r = a(\tau)\chi$  in Eq.18. This is illustrated in Fig.5. In this case we need to distinguish between two different effective  $\rho_\Lambda$ , the one in the inside FLRW metric,  $\rho_{\Lambda_{\text{in}}}$  and the one for the outside background,  $\rho_{\Lambda_{\text{out}}}$ , which should be smaller (see Appendix A). This is independent of  $\Lambda$ , which is always fixed (see Appendix C).

The solutions to the field equations are independent of the choice of coordinates but  $\tilde{T}_{\mu\nu}(t, r)$  depends on the fluid motion (see Eq.34). We used comoving coordinates  $(\tau, \chi)$ , where the fluid is expanding

and the observed is comoving, to find the interior solution. But we can then transform back to proper SW frame  $(t, r)$ , using the duality transformation Eq.26, to find a full BH solution in Eq.33 that is continuous in the metric and curvature at  $r_{SW}$ , like in the BH.fv case. As in the singular BH.SW metric, outgoing radial null geodesics cannot escape the event horizon, but incoming ones can enter (see discussion around Eq.15). So the BHU solution is a physical BH.

### 6.3 BH formation

Another issue, which we only address partially in §2.1, is how such physical BH solutions can be achieved (e.g. astrophysical and primordial BH formation) and if they can have a causal origin. There is extensive literature on Bubble Universe formation (e.g. see Garriga et al. 2016; Oshita & Yokoyama 2018 and references) but they typically involve quantum gravity ideas or extensions. Hubble dumping of the kinetic energy  $K$  of a classical scalar field  $\varphi$  (see Fig.1) can result in a FV trapped field configuration. Such initially small local discontinuity, with FV energy density  $\Delta$ , will grow as Eq.42 until it reaches the stable BH size corresponding to  $\rho_{BH} = \Delta$ . So  $\Delta$  is the BH density: the smaller  $\Delta$  the larger the BH size and mass. As illustrated in Fig.1 if we think of  $V(\varphi)$  as the superposition of many plane waves of different frequencies this will result in a landscape of nested BHU of different masses and sizes.

Could a BHU formed just from the final collapse of a dying star? Instead of a forming a BH.SW singularity (as usually assumed), such stellar collapse may just result into a large supernova (SN) explosion. As pointed out by Buchdahl (1959), regular matter can only be compressed to a radius which is 9/8 times larger than that of BH.SW, so such explosion seems unavoidable if the collapse does not halt before (forming a more compact object). As explained above, during the SN explosion, Hubble damping of the kinetic energy associated to a local scalar field  $\varphi$  could result into a trapped FV, which will grow into BH.fv and can also produce matter/radiation (from reheating) and turn into a BH.u.

Matter and radiation can also infall into a BH. For a BH.SW solution we assume that this results into a BH mass increase. But for a BHU this results in a jump of the internal Hubble expansion rate ( $\Delta H/H = M_1/(2M_2)$ ). Such jump will be diluted away in time by the same accelerated expansion. So whatever we feed a BHU with, it is lost into internal kinetic expanding energy with no change in the BH mass, which is given by the FV energy. In Fig.1 we can see that BHU of very different masses can be formed as the spectrum of  $\Delta_i$  values could be quite broad if we allow  $V(\varphi)$  to be a superposition of many plane waves.

These ideas are speculative as we need a detailed modeling to find how all this happens. But the point we want to make here is that the BH interior seems important for models of BH formation and we can not just assume that a BH corresponds to a singular BH.SW metric inside, because this is not a physical solution. We conclude that further work is needed to understand BH formation.

### 6.4 What is $M$ for a physical BH?

For a stellar or galactic BH within a larger universe where we neglect  $\Lambda$  or  $V_0$ , the BH mass  $M$  in the BHU is given by the FV excess energy  $\Delta$ , so that  $\rho_{BH}$  in Eq.1 is  $\rho_{BH} = \Delta$  and  $M = (32\pi G^3 \Delta/3)^{-1/2}$ . For a more general case see Eq.B3. So the larger  $\Delta$  the smaller the BH mass and size. This is independent of the matter and energy content that falls inside the BH. So  $M$  in the BHU solution does not correspond to the actual total mass or radiation inside, which is not observable

from the outside, but should instead be interpreted in terms of the FV energy excess  $\Delta$ . This could have implications for models of astrophysical BH formation (such as Kormendy & Ho 2013) and primordial BH formation (e.g. Kusenko 2020 and references therein) which usually assume that BH accretion and merging results in linear increase of the BH mass  $M$ .

### 6.5 Our universe as a BH

Both BH type solutions can be interpreted as a BH within our universe or as an expanding universe inside a larger space-time. As pointed out in the introduction, that the universe might be generated from the inside of a BH has a long and interesting history. Knutsen (2009) argued that  $p$  and  $\rho$  in the homogeneous FLRW solution are only a function of time (in comoving coordinates) and can not change at  $r = r_{SW}$  to become zero in the exterior. This is an important point and seems to contradict the BHU solution. The riddle is resolved with  $\Lambda$ . Without  $\Lambda$  the FLRW universe can not have a causal origin: the comoving density and Hubble rate are the same everywhere, and this is not causally possible. A causal horizon  $\chi_\S$  fixes  $\Lambda$  (Gaztañaga 2021) which solves this problem and also generates an even horizon  $\chi_\S = r_{SW}$  similar to that of a BH.SW:  $r_{SW}$ . This allows for an homogeneous FLRW solution inside  $r_{SW}$  that has a  $\rho_\Lambda$  discontinuity at  $r_{SW}$  and looks in-homogeneous in the SW frame.

Homogeneity is therefore the illusion of the comoving observer inside  $r_\Lambda = r_{SW}$ . The FLRW metric is trapped inside  $r < r_\Lambda$ , and is then equivalent to an inhomogeneous spherically symmetric metric of Eq.28. The FLRW metric is only homogeneous in space, but not in space-time. A new frame where comoving time and space are mixed, can break or restore this symmetry. The frame duality in Eq.26 is only valid for proper coordinates that are centered at the BH location. But in the transformed (comoving) frame any point inside the BHU is subject to the same expansion law with equal  $a(\tau)$ . From every point inside de BHU, observers will see an homogeneous and isotropic space-time around them. Just like in the universe around us.

### 6.6 Evidence for a BHU

We can sketch the evolution of our universe with this BHU model (see Fig.3-4). In proper coordinates this solution has no BB (or bounce): it is not singular at  $r = 0$  or at  $\tau = 0$ , because we have a non-singular BH.fv before we start the FLRW BH.u phase. The inside comoving observer is trapped inside  $r < r_{SW} = 2GM = 1/H_\Lambda$  and has the illusion of a BB. The space-time outside (the parent FLRW universe) could be longer and larger than the BB estimates. We could have a network of island universes with matter and radiation in between.

This also explains why our universe (or other island universes) is expanding and not contracting. The initial fluctuation  $H_i^2 = 8\pi G\Delta/3$  could be expanding ( $H_i > 0$ ) or contracting ( $H_i < 0$ ). In the later case it will either recollapse very quickly or it will else bounce into expansion dominated by the repulsive gravitational force that results from the negative pressure from constant  $\Delta$  or  $\Lambda$  (see Eq.44).

We have other observational evidence that the expanding metric around us is inside a BHU. We can recover the BB homogeneous solution in the limit  $\Delta \Rightarrow 0$ , where we have  $r_{SW} \Rightarrow \infty$  and  $\rho_\Lambda = 0$ . But we have measured  $\rho_\Lambda > 0$  ( $\Omega_\Lambda \simeq 0.7$ ) which implies  $M \simeq 5.8 \times 10^{22} M_\odot$  and  $r_{SW} \simeq c/H_0$ , as in the BHU. The causal interpretation for  $\chi_\S$ , also explains the observed coincidence between  $\rho_\Lambda$  and  $\rho_m$  today (Gaztañaga 2020; Gaztañaga 2021). See also Appendix C about the coincidence problem and the causal boundary.

If we look back to the CMB times,  $\chi_\S$  corresponds to  $\simeq 60$  degrees in the sky. The observed anomalies in the CMB temperature

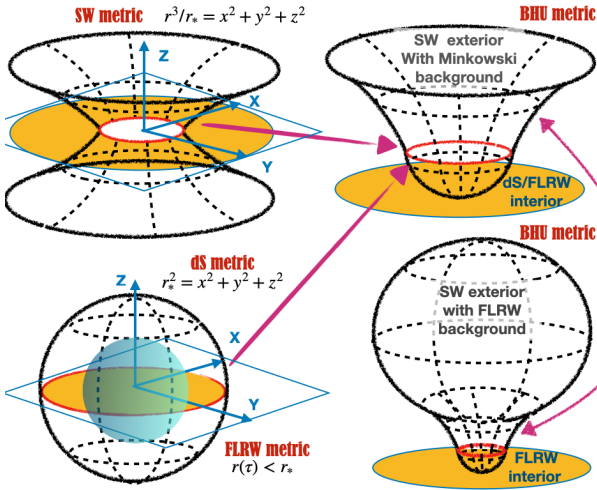


**Figure 5.** Spatial representation of  $ds^2 = (1+2\Phi)^{-1}dr^2 + r^2d\theta^2$  2D metric embedded in 3D flat space for: deSitter (dS, bottom left,  $2\Phi = -r^2/r_*^2$ ), FLRW ( $r(\tau) < r_*$ , blue sphere inside dS), Schwarzschild (SW, top left,  $2\Phi = -r_*/r$ ) and two versions of the combined BHU metrics. Yellow region shows the projection coverage in the  $(x, y)$  plane. In the top right figure we show a BHU with dS (or FLRW) interior and SW metric exterior joint at the Event Horizon  $r_* = 2GM = 1/H_\Lambda$  (red circles). The BHU solution has in general two nested FLRW metrics join by SW metric (bottom right). See Appendix A.

maps at larger scales (Gaztañaga 2020; Gaztañaga 2021; Fosalba & Gaztañaga 2021; Gaztañaga & Fosalba 2021) provide additional support for the anisotropies expected in the BHU model. There is also a window to see outside our BHU using the largest angular scales for  $z > 2$  and measurements of cosmological parameters from very different cosmic times. There is already mounting evidence for this (e.g. Planck Collaboration 2020; Riess 2019; Abbott et al. 2019).

If there are other island universes outside ours, Galaxies and QSO, as well as BHs, could be accreted from outside  $r_\Lambda$  into our BHU. Because the horizon  $1/H_\Lambda$  is so large, we can only see evidence of those mergers at early times, during or right after the CMB, when  $\chi_8$  subtends  $\approx 60$ deg. on the sky. Could this be related to rarely old QSO or galaxies observed at high  $z$ ? If our BHU merges with another BHU which is few % smaller, we might be able to see such % glitches in  $H(z)$  with current or future data, at  $z > 2$  and very large angle separation.

Camacho & Gaztañaga (2021) found evidence for homogeneity and lack of correlations in the CMB at  $r > r_\Lambda$ . This suggests that the underlying physical mechanism sourcing the observed anisotropy encompasses scales beyond our causal universe. Fosalba & Gaztañaga (2021) found variations in cosmological parameters over large CMB regions. This is the largest reported evidence for a violation of the Cosmological principle. Such observations indicate a breakdown of the standard BB picture in favor of the BHU. Their Fig.31 shows that the size of these regions follow the BHU relation between  $\chi_8$  and  $\rho_\Lambda$ . This is consistent with the idea that our universe was accreted to or created by a larger BHU.

## ACKNOWLEDGMENTS

I want to thank Marco Bruni, Robert Caldwell, Alberto Diez-Tejedor and Angela Olinto for their feedback. This work has been supported by spanish MINECO grants PGC2018-102021-B-100 and EU grants

LACEGAL 734374 and EWC 776247 with ERDF funds. IEEC is funded by the CERCA program of the Generalitat de Catalunya.

## References

- Abbott T. M. C., et al., 2019, *Phys. Rev. Lett.*, **122**, 171301  
Aguirre A., Johnson M. C., 2005, *Phys. Rev. D*, **72**, 103525  
Albrecht A., Steinhardt P. J., 1982, *Phys. Rev. Lett.*, **48**, 1220  
Blau S. K., Guendelman E. I., Guth A. H., 1987, *Phys. Rev. D*, **35**, 1747  
Bondi H., Gold T., 1948, *MNRAS*, **108**, 252  
Brustein R., Medved A. J. M., 2019, *Phys. Rev. D*, **99**, 064019  
Buchdahl H. A., 1959, *Phys. Rev.*, **116**, 1027  
Camacho B., Gaztañaga E., 2021, arXiv e-prints, p. arXiv:2106.14303  
Dadhich N., 2007, *Pramana*, **69**, 23  
Daghighi R. G., Kapusta J. I., Hosotani Y., 2000, arXiv:gr-qc/0008006,  
Díez-Tejedor A., Feinstein A., 2006, *Phys. Rev. D*, **74**, 023530  
Dymnikova I., 2003, *International Journal of Modern Physics D*, **12**, 1015  
Dymnikova I., 2019, *Universe*, **5**, 111  
Dyson L., Kleban M., Susskind L., 2002, *J. of High Energy Phys*, **2002**, 011  
Easson D. A., Brandenberger R. H., 2001, *J. of High Energy Phys.*, **2001**, 024  
Ellis G., 2008, *Astronomy and Geophysics*, **49**, 2.33  
Ellis G., Silk J., 2014, *Nature*, **516**, 321  
Firouzjahi H., 2016, arXiv e-prints, p. arXiv:1610.03767  
Fosalba P., Gaztañaga E., 2021, *MNRAS*, **504**, 5840  
Frolov V. P., Markov M. A., Mukhanov V. F., 1989, *Phys Let B*, **216**, 272  
Galtsov D. V., Lemos J. P., 2001, *Classical and Quantum Gravity*, **18**, 1715  
Garriga J., Vilenkin A., Zhang J., 2016, *JCAP*, **2016**, 064  
Gaztañaga E., 2020, *MNRAS*, **494**, 2766  
Gaztañaga E., 2021, *MNRAS*, **502**, 436  
Gaztañaga E., Fosalba P., 2021, p. arXiv:2104.00521  
Good I. J., 1972, *Physics Today*, **25**, 15  
Guth A. H., 1981, *Phys. Rev. D*, **23**, 347  
Hoyle F., 1948, *MNRAS*, **108**, 372  
Israel W., 1967, *Nuovo Cimento B Serie*, **48**, 463  
Kaloper N., Kleban M., Martin D., 2010, *Phys. Rev. D*, **81**, 104044  
Knutsen H., 2009, *Gravitation and Cosmology*, **15**, 273  
Kormendy J., Ho L. C., 2013, *ARA&A*, **51**, 511  
Kusenko A. e., 2020, *Phys. Rev. Lett.*, **125**, 181304  
Landsberg P. T., 1984, *Annalen der Physik*, **496**, 88  
Linde A. D., 1982, *Physics Letters B*, **108**, 389  
Mazur P. O., Mottola E., 2015, *Classical and Quantum Gravity*, **32**, 215024  
Misner C. W., Thorne K. S., Wheeler J. A., 1973, *Gravitation*  
Mitra A., 2012, *Nature Sci. Reports*, **2**, 923  
O’Raifeartaigh C., Mitton S., 2015, p. arXiv:1506.01651  
Oshita N., Yokoyama J., 2018, *Physics Letters B*, **785**, 197  
Padmanabhan T., 2010, *Gravitation*, Cambridge Univ. Press  
Pathria R. K., 1972, *Nature*, **240**, 298  
Penrose R., 2006, Conf. Proc. C, 060626, 2759  
Planck Collaboration 2020, *A&A*, **641**, A6  
Popławski N., 2016, *ApJ*, **832**, 96  
Riess A. G., 2019, *Nature Reviews Physics*, **2**, 10  
Smolin L., 1992, *Classical and Quantum Gravity*, **9**, 173  
Starobinskiĭ A. A., 1979, *Soviet J. of Exp. and Th. Physics Letters*, **30**, 682  
Stuckey W. M., 1994, *American Journal of Physics*, **62**, 788  
Zhang T. X., 2018, *Journal of Modern Physics*, **9**, 1838

## APPENDIX A: GEOMETRICAL REPRESENTATIONS

To visualize the BHU metric in a 2D plot we consider the most general shape for a spherically symmetric metric in 2D space  $(x, y)$  embedded in 3D flat space  $(x, y, z)$ . In polar coordinates  $(r, \theta)$  with  $r^2 = x^2 + y^2$  and  $\tan \theta = x/y$  we have:

$$ds^2 = \frac{dr^2}{1+2\Phi} + r^2d\theta^2 \quad (\text{A1})$$



In 3D space we just have one additional angle,  $\delta$ , in Eq.16, but the radial part is the same. The case  $\Phi = 0$  corresponds to flat space:  $ds^2 = dx^2 + dy^2$ . The simplest case with curvature can be represented by a 2D sphere (S2) embedded in 3D flat space using an extra dimension  $z$ :

$$ds^2 = dx^2 + dy^2 + dz^2 \quad ; \quad x^2 + y^2 + z^2 = r_*^2 \quad (\text{A2})$$

This metric is flat in 3D coordinates, but constraint to  $r_*$ , which is the radius of the sphere and the curvature within the 2D surface of S2. We can replace  $z$  by  $r$  using:  $z^2 = r_*^2 - r^2$  to find:

$$ds^2 = dx^2 + dy^2 + dz^2 = \frac{dr^2}{1 - r^2/r_*^2} + r^2 d\theta^2 \quad (\text{A3})$$

so that  $2\Phi = -r^2/r_*^2$  just like in the dS metric of Eq.23 for  $r_* = r_\Lambda$ . It tell us that dS space corresponds to being in the flat surface of a sphere (like us in Earth). This is illustrated in the bottom left of Fig.5. Note how  $(r, \theta)$  are coordinates in the  $(x, y)$  plane. The S2 space is trapped or bounded by  $r < r_*$  (yellow region). The metric changes signature (becomes imaginary) for  $r > r_*$ : this region of space does not exist (white region). The case  $r = r_*$  (red circles) corresponds to the Event Horizon at  $2\Phi = -1$ .

The Newtonian interpretation of  $2\Phi = -r^2/r_*^2$  is that this is caused by a centrifugal force, like that in the orbit of a satellite. Even when there is no matter, the curvature (or boundary) is interpret as a repulsive gravitational force that causes acceleration.

The FLRW metric (or dSE metric in Eq.28) correspond to a smaller sphere S2 (inside dS sphere) with an expanding radius  $r_H(\tau)$  that tends asymptotically to  $r_\Lambda = 1/H_\Lambda$  (see Eq.28):

$$ds^2 = dx^2 + dy^2 + dz^2 \quad ; \quad x^2 + y^2 + z^2 = r_H^2(\tau) \quad (\text{A4})$$

So it has the same topology and Event Horizon or trapped surface (red circle) as dS metric. It is represented in Fig.5 by a blue sphere inside dS sphere in the bottom left corner. This illustrates how it is possible that each observer inside sees an homogeneous space even when the sphere is centered around a given position.

The next simplest case can be represent by a static radius that increases with  $r$ :

$$ds^2 = dx^2 + dy^2 + dz^2 \quad ; \quad x^2 + y^2 + z^2 = r^3/r_* \quad (\text{A5})$$

As before, we can replace  $z$  by  $r$  using:  $z^2 = r^3/r_* - r^2$  to find:

$$ds^2 = dx^2 + dy^2 + dz^2 = \frac{dr^2}{1 - r/r_*} + r^2 d\theta^2 \quad (\text{A6})$$

so that  $2\Phi = -r_*/r$  just like in the SW metric of Eq.22 for  $r_* = 2GM$ . This is illustrated in the top left of Fig.5. The case  $r = r_*$  (red circle) corresponds to the Event Horizon at  $2\Phi = -1$ . The Newtonian interpretation for  $2\Phi = -r_*/r$  is the inverse square law for a point mass  $M$ :  $r_* = 2GM$ .

The SW space is bounded by  $r > r_*$  (yellow region). The metric changes signature (becomes imaginary) for  $r < r_*$ . Contrary to many other representations of SW metric, it is clear here that this inner region of space does not exist (it is not covered by the metric in actual space). This coverage is complementary to dS or FLRW metric which cover the inner region and not the outer region. We can match the dS and SW metrics at  $r = r_*$  to cover the full  $(x, y)$  plane as in the BHU metric. Physically this corresponds to a balance between the centrifugal force, represented by dS potential  $2\Phi = -r^2/r_*$ , and the SW inverse square law,  $2\Phi = -r_*/r$ , like what happens in the circular Keplerian orbits.<sup>2</sup>

This BHU metric is shown in the top right of Fig.5, which is asymptotically Minkowski. The dS metric is the limiting case of FLRW metric and SW metric is a perturbation over FLRW metric. So more generally, the BHU is a combination of 2 FLRW metrics join by a SW metric. The junction happens at the effective value of  $r_* = r_\Lambda = 2GM$  corresponding to the inner FLRW  $\rho_\Lambda$  (which we denote as  $\rho_{\Lambda_{in}}$ ). If the outter FLRW has  $\rho_{\Lambda_{out}} \neq 0$ , then the SW hyperbolic surface will close as another S2 sphere (bottom right). If  $\rho_{\Lambda_{out}} = 0$  we have asymptotic Minkowski space (top right).

## APPENDIX B: SOLUTION FOR $V_0 \neq 0$ AND $\Lambda \neq 0$

Eq.30 for  $V_0 \neq 0$  and  $\Lambda \neq 0$ :

$$\rho(r) = \begin{cases} V_0 & \text{for } r > r_{SW} \\ V_0 + \Delta & \text{for } r < r_{SW} \end{cases} \quad (\text{B1})$$

can be solved as  $\Phi = \Psi$  with

$$2\Phi = \begin{cases} -r_{SW}/r - r^2 H_{\Lambda_{out}}^2 & \text{for } r > r_{SW} \equiv 2GM(1 + \epsilon) \\ -r^2 H_{\Lambda_{in}}^2 & \text{for } r < r_{SW} = r_{\Lambda_{in}} \equiv 1/H_{\Lambda_{in}} \end{cases} \quad (\text{B2})$$

where  $\epsilon \equiv \rho_{\Lambda_{out}}/\Delta$  and

$$3H_{\Lambda_{out}}^2 \equiv 8\pi G \rho_{\Lambda_{out}} \quad ; \quad \rho_{\Lambda_{out}} = \Lambda/8\pi G + V_0 \quad (\text{B3})$$

$$3H_{\Lambda_{in}}^2 \equiv 8\pi G \rho_{\Lambda_{in}} \quad ; \quad \rho_{\Lambda_{in}} = \rho_{\Lambda_{out}} + \Delta \quad (\text{B4})$$

So there are different effective  $\rho_\Lambda$  outside ( $\rho_{\Lambda_{out}}$ ) and inside ( $\rho_{\Lambda_{in}}$ ). The exterior of the BH has the dSW metric but more generally it is a perturbation of the FLRW metric.

## APPENDIX C: THE COINCIDENCE PROBLEM

Consider our Universe as the interior of a BHU. For a universe of finite age, there is finite causal boundary M. This requires a boundary term for the action that fixes  $\Lambda = 4\pi G < \rho + 3p >$ , where the average is over the light-cone inside M (Gaztañaga 2021). If the causal boundary is set to  $M = M_I + M_O$ , where  $M_I$  and  $M_O$  are the volumes inside and outside the BHU, we find:

$$\frac{\Lambda}{4\pi G} = < \rho + 3p > = -2V_0 - 2\Delta \frac{M_I}{M} + < \rho_m + 2\rho_R > \quad (\text{C1})$$

We then have that  $\rho_{\Lambda_{in}} = V_0 + \Delta + \Lambda/8\pi G$  becomes:

$$\rho_{\Lambda_{in}} = \begin{cases} \Delta & \text{for } M_O \gg M_I \\ < \rho_m/2 + \rho_R > & \text{for } M_I \gg M_O \end{cases} \quad (\text{C2})$$

The first case corresponds to a small BHU inside a larger space where  $< \rho_m/2 + \rho_R > \simeq 0$  because the BHU content is negligible when average over a much larger outside volume  $M_O$ . This also represents a BH inside our Universe. The second case corresponds to a BHU that is causally disconnected from the rest of space-time. The observational fact that  $\rho_\Lambda \sim \rho_m$  seems to agree well with this second solution (Gaztañaga 2021). This agreement (the coincidence problem) seems to be telling us that the light-cone volume outside our BHU is not very large. But note that  $< \rho_m/2 + \rho_R > \simeq \Delta$  if matter and radiation are generated by some reheating (see §2.1). DE, inflation and BH interior seem different aspects of the same BHU solution.

<sup>2</sup> See: <https://darkcosmos.com/home/f/keplers-laws>.